

GEOLOGIC MAPPING INVESTIGATIONS OF THE NORTHWEST RIM OF HELLAS BASIN, MARS.

David A. Crown¹, Leslie F. Bleamaster III¹, Scott C. Mest¹, John F. Mustard², and Mathieu Vincendon², ¹Planetary Science Institute, 1700 E. Ft. Lowell Rd., Suite 106, Tucson, AZ 85719; crown@psi.edu, ²Dept. of Geological Sciences, Brown University, Providence, RI 02912.

Introduction: The Hellas impact basin, spanning 2000+ km in the cratered highlands, is the largest well-preserved impact structure on Mars and its deepest depositional sink. The Hellas region is significant for evaluating Mars' hydrogeologic and climate histories, given the nature, diversity, and range in ages of potential water- and ice-related landforms [e.g., 1-2], including possible paleolakes on the basin floor [2-4]. The circum-Hellas highlands are of special interest given recent studies of potential localized fluvial/lacustrine systems [2, 5-17] and evidence for phyllosilicates around and within impact craters north of the basin [18-26].

Study Area and Mapping Objectives: Our current studies examine the evolution of Hellas' NW rim where basin floor deposits transition abruptly to the cratered highlands. We are producing a 1:1.5M-scale geologic map of eight MTM quadrangles (-25312, -25307, -25302, -25297, -30312, -30307, -30302, -30297) along Hellas' NW rim. The map region (22.5-32.5°S, 45-65°E) includes a transect across the cratered highlands of Terra Sabaea, the degraded NW rim of Hellas, and basin interior deposits of northwestern Hellas Planitia. No previous mapping studies have focused on this region, although it has been included in earlier global and regional maps [27-29]. Geologic mapping of the NW Hellas rim is providing new constraints on the magnitudes, extents, and history of volatile-driven processes as well as a geologic context for mineralogic identifications.

Geologic Mapping: Research to-date [30-32] has included general terrain characterization and comparison to other circum-Hellas regions, preliminary evaluation of geomorphology and stratigraphic relationships, preliminary exploration of compositional signatures using CRISM, and investigation of impact crater distribution, morphometry, and interior deposits, as well as production of a preliminary geologic map of part of the map area.

Hellas NW Rim Geology. The NW Hellas rim can be divided into four physiographic zones: 1) Terra Sabaea highlands (above 500m), 2) Terra Sabaea plains (-1800m - 500m), 3) Hellas rim (-5800m - -1800m), and 4) Hellas floor (below -5800m). All of these zones show significant numbers of moderate to large impact craters, suggesting that the basic geologic framework of the region was established early in Martian history with the formation of densely cratered

terrains. The zones show clear differences in the types of landforms and materials exposed as well as differences in crater degradation states. A significant and complex sedimentary history can be inferred given that many large craters have been infilled and expose layered interior deposits, as well as by numerous scarps and valleys within intercrater plains.

The densely cratered highlands of Terra Sabaea contain impact craters of a wide range in size and that display a variety of degradation styles and states. Crater interiors and local, low-lying regions of the intercrater plains may be depositional sites for aeolian, fluvial, and/or lacustrine sediments.

The characteristics of the Terra Sabaea plains suggest lowering of the highland surface and creation of a younger shelf separating Terra Sabaea proper from the steeper basin rim zone. In THEMIS images, the plains in this zone show abundant scarps, a variety of subunits, and a multitude of surface variations. The zone, or shelf, appears to be part of a larger shelf along Hellas' northern rim and is located at elevations similar to those that exhibit smooth and channeled plains along Hellas' east rim [i.e., 2]. The east rim is interpreted to be a large depositional shelf potentially associated with flooding from Reull Vallis, large paleolakes within Hellas, and/or accumulation of atmospheric volatiles due to circulation patterns off of the south pole [e.g., 2, 4, 33-34].

The Hellas rim and floor zones exhibit buried and softened landforms as well as small valleys. In several locations, valley segments appear to form disconnected downslope patterns. Small lobate debris aprons are observed extending from local topographic highs. Layered surficial deposits are also evident.

Preliminary Mapping Results. Geologic mapping of a test region (22.5-29°S, 57.6-65°E) of NW Hellas indicates that surface materials can be divided into the following types: highlands, smooth plains, and crater floor deposits. Mapping shows an eroded and extensively buried ancient highland landscape, with partial exhumation indicated by etched surfaces and retreat of plains around eroded massifs and crater rims (Figs. 1, 2) [32]. Small valleys dissect the plains surface and are concentrated on sloping plains deposits at the margins of highland outcrops. Detailed mapping of this sub-region has resulted in the identification of a larger number of irregular depressions than was found in the initial survey of the entire study area [30]. In some cases the scarps defining these depressions

reveal finely layered outcrops. The occurrence of the irregular depressions and layered outcrops in both crater floor deposits and within the plains may indicate emplacement of sedimentary units on a regional scale.

Multispectral mapping with CRISM. Central to our investigation are compositional characterizations using MRO CRISM data. We have analyzed CRISM multispectral data for the NW Hellas map area for phyllosilicates and Fe-silicates (olivine-pyroxene). Fe/Mg phyllosilicate minerals (e.g., saponite, chlorite) are recognized on the basis of narrow absorption features between 1.8 and 2.4 μm . Phyllosilicates are typically observed in association with crater rims and massifs, but also are evident in some crater ejecta and floor deposits (Fig. 3), as for Tyrrhena Terra in general [26]. We are integrating these mineralogic results into our geologic mapping analyses.

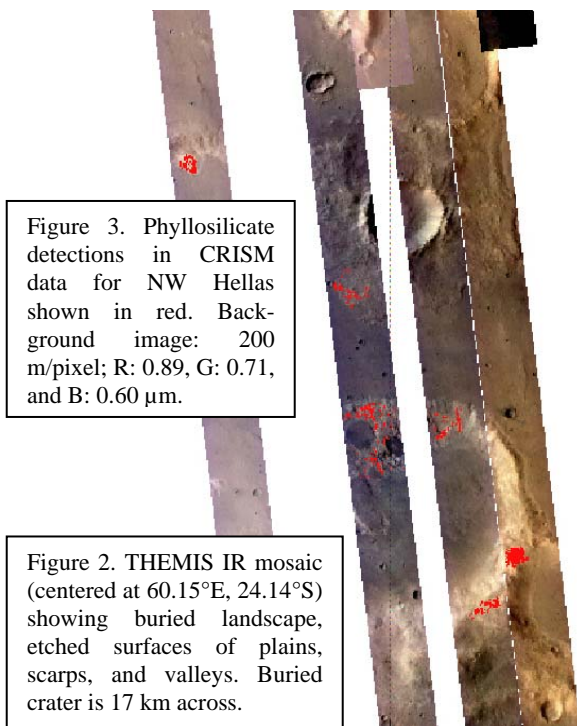


Figure 3. Phyllosilicate detections in CRISM data for NW Hellas shown in red. Background image: 200 m/pixel; R: 0.89, G: 0.71, and B: 0.60 μm .



Figure 2. THEMIS IR mosaic (centered at 60.15°E, 24.14°S) showing buried landscape, etched surfaces of plains, scarps, and valleys. Buried crater is 17 km across.

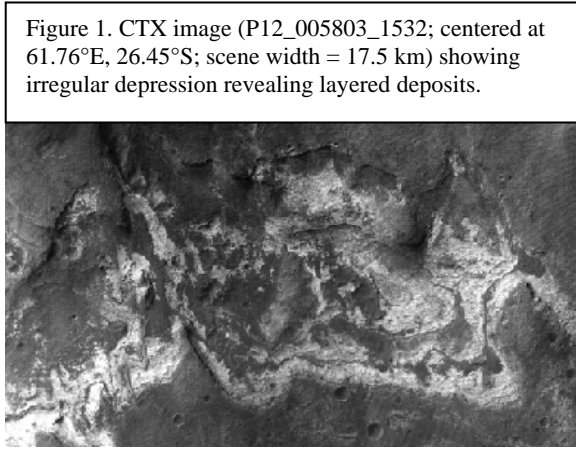


Figure 1. CTX image (P12_005803_1532; centered at 61.76°E, 26.45°S; scene width = 17.5 km) showing irregular depression revealing layered deposits.

References: [1] Tanaka, K.L. and G.J. Leonard (1995), *JGR*, 100, 5407-5432. [2] Crown, D.A. et al. (2005), *JGR*, 110, E12S22, doi:10.1029/2005JE002496. [3] Moore, J.M. and D.E. Wilhelms (2001), *Icarus*, 154, 258-276. [4] Bleamaster, L.F. and D.A. Crown (2009), in USGS edit. [5] Lahtela, H. et al. (2003), *Vernadsky Institute-Brown University Microsymposium 38*, MS057. [6] Lahtela, H. et al. (2005), *LPSC XXXVI*, abstract 1683, LPI (CD-ROM). [7] Ansan, V. and N. Mangold (2004), 2nd Conf. on Early Mars, abstract 8006, LPI (CD-ROM). [8] Ivanov, M.A. et al. (2005), *JGR*, 110, E12S21, doi:10.1029/2005JE002420. [9] Kortenienmi, J. et al. (2005), *JGR*, 110, E12S18, doi:10.1029/2005JE002427. [10] Kraal, E.R. et al. (2005), *Role of Volatiles on Martian Impact Craters*, abstract 3008, LPI (CD-ROM). [11] Mest, S.C. and D.A. Crown (2005), *Icarus*, 175(2), 335-359. [12] Mest, S.C. (2005), *Role of Volatiles on Martian Impact Craters*, abstract 3014, LPI (CD-ROM). [13] Mest, S.C. (2006), *LPSC XXXVII*, abstract 2236, LPI (CD-ROM). [14] Moore, J.M. and A.D. Howard (2005), *JGR*, 110, E04005, doi:10.1029/2004JE002352. [15] Moore, J.M. and A.D. Howard (2005), *LPSC XXXVI*, abstract 1512, LPI (CD-ROM). [16] Wilson, S.A. and A.D. Howard (2005), *LPSC XXXVI*, abstract 2060, LPI (CD-ROM). [17] Wilson, S.A. et al. (2007), *JGR*, 112, E08009, doi:10.1029/2006JE002830. [18] Poulet, F. et al. (2005), *Nature*, 438, 623-627. [19] Bibring, J.-P. et al. (2006), *Science*, 312, 400-404. [20] Costard, F. et al. (2006), *LPSC XXXVII*, abstract 1288, LPI (CD-ROM). [21] Murchie, S. et al. (2006), *EOS Trans. AGU*, abstract P33A-04. [22] Murchie, S. et al. (2007), *JGR*, 112, E05S03, doi:10.1029/2006JE002682. [23] Mustard, J.F. et al. (2007), *LPSC XXXVIII*, abstract 2071, LPI (CD-ROM). [24] Mustard, J.F. et al. (2007), 7th Inter. Conf. on Mars, LPI. [25] Pelkey, S.M. et al. (2007), *LPSC XXXVIII*, abstract 1994, LPI (CD-ROM). [26] Pelkey, S.M. et al. (2007), *JGR*, 112, E08S14, doi:10.1029/2006JE002831. [27] Scott, D.H. and M.H. Carr (1978), *USGS Misc. Invest. Ser. Map*, I-1083. [28] Greeley, R. and J.E. Guest (1987), *USGS Misc. Invest. Ser. Map* I-1802B. [29] Leonard, G.J. and K.L. Tanaka (2001), *USGS Geol. Invest. Ser. Map* I-2694. [30] Crown, D.A. et al. (2007), *EOS Trans. AGU*, abstract P41A-0189. [31] Mest, S.C. et al. (2008), *LPSC XXXIX*, abstract 1704, LPI (CD-ROM). [32] Crown, D.A. et al. (2009), *LPSC XL*, abstract 1705, LPI (CD-ROM). [33] Colaprete, A. et al. (2004), *LPSC XXXV*, abstract 2149, LPI (CD-ROM). [34] Colaprete, A. et al. (2005), *Nature*, 435, 184-188.